Modelling human balance using switched systems with linear feedback control

Kowalczyk, Piotr and Glendinning, Paul and Brown, Martin and Medrano-Cerda, Gustavo and Dallali, Houman and Shapiro, Jonathan

2011

MIMS EPrint: **2010.81**

Manchester Institute for Mathematical Sciences
School of Mathematics

The University of Manchester

Reports available from: http://eprints.maths.manchester.ac.uk/
And by contacting: The MIMS Secretary
School of Mathematics
The University of Manchester
Manchester, M13 9PL, UK

ISSN 1749-9097

Modelling human balance using switched systems with linear feedback control

Piotr Kowalczyk [*], Paul Glendinning [†], Martin Brown [‡], Gustavo Medrano-Cerda [§], Houman Dallali [¶] and Jonathan Shapiro [‖]

April 7, 2011

Abstract

We are interested in understanding the mechanisms behind and the character of the sway motion of healthy human subjects during quiet standing with eyes closed. We assume that a human body can be modelled as a single-link inverted pendulum, and the balance is achieved using liner feedback control. Using these assumptions we derive a switched model which we then investigate. Stable periodic motions (limit cycles) about an upright position are found. The existence of these limit cycles is studied as a function of system parameters. The exploration of the parameter space leads to the detection of multistability and homoclinic bifurcations.

1 Introduction

In spite of recent advances in revealing the mechanisms responsible for balancing during quiet standing (see for instance [1, 2, 3, 4, 5, 6, 7, 8, 9, 10, 11]) the physiological mechanisms are far from being understood. In recent years there has been a growing interest among scientists to use mathematical modelling and numerical simulations to gain new insights into the problem of balancing. In the literature it has been argued that forward body sway can be captured using models where the muscles and tendon-muscle complexes act as springs with certain stiffness and the neuromuscular system generates the corrective torque [12, 13, 14, 15]. Models based on these assumptions have been tested experimentally [13, 12, 16, 8]. In [16, 8] a single-link inverted pendulum model with

[*] *Corresponding Author.* School of Computing, Mathematics and Digital Technology, John Dalton Building, Manchester Metropolitan University, Chester Street, Manchester, M1 5GD, U.K., Tel. +44(0)161 247 1136, E-mail: p.kowalczyk@mmu.ac.uk

[†] School of Mathematics, The University of Manchester, Oxford Road, Manchester M13 9PL, U.K., Tel. +44(0)161 3068972, Fax +44(0)161 306 3669, E-mail: p.a.glendinning@manchester.ac.uk

[‡] School of Electrical and Electronic Engineering, The University of Manchester Manchester, M13 9PL, U.K., Tel. +44(0)161 3064672, E-mail: Martin.Brown@manchester.ac.uk

[§] Gustavo A Medrano-Cerda, Istituto Itialiano di Tecnologia, Genova, Italy

[¶] School of Mathematics, The University of Manchester, Oxford Road, Manchester M13 9PL, U.K., Tel. +44(0)161 3063214, Fax +44(0)161 306 3669, E-mail: Houman.Dallali@postgrad.manchester.ac.uk

[‖] School of Computer Science, The University of Manchester, Manchester, M13 9PL, U.K., Tel. +44(0)161 275 6253, E-mail: jonathan.l.shapiro@manchester.ac.uk

simple linear feedback was introduced. Different feedback laws were considered to obtain the best match to experimental data, and it was shown that a corrective torque proportional to the position and velocity signals combined with time delays can be used to account for the body sway observed experimentally.

Early work [17] suggested that intermittent control plays an important role in human motor control. Recent research [18, 19] shows that intermittent control is a mechanism that can explain the results found in experimental tests. However, the authors also point out that there are alternative control models that can reproduce experimental results. Further research is needed to design experimental tests that can help to discriminate between different control models. An alternative model for human postural sway was considered in [20]. In this work the authors use a reduced first order model with a time delayed feedback. This model is an approximation of the second order inverted pendulum model valid for healthy subjects with eyes open. In place of intermittent control, [20] considers a switched control system depending on a threshold for the angular position. For the first order model, [20] shows the existence of bi-stable limit cycles. In [21, 22] the switch-like balance controller was considered as a type of intermittent control. The idea of switched control was further explored in [23, 24]. The authors considered a model with switched control, random perturbations that model noise, and time delay. It was shown that the interplay between noise and time delay may have a stabilising property. The authors also argued that the control applied by humans is an adaptive switched control. The idea of switched control applied by humans during quiet standing serves as a starting point for the modelling approach adopted in the current paper.

We approach the problem of human balancing by considering the subjects standing on both legs with eyes closed or open. We are interested in investigating the sway motion that occurs in the sagittal plane, i.e., we consider a forward-backward body sway.

The following assumptions are made:

- The body control is achieved using proprioception only (reception of internal signals such as posture and body sway through the length and elongation velocity of the muscles);
- We include time delays in the control system that represent the combined delays due to sensory reception, neural transmission, neural processing, muscle activation, and force development of the proprioception motor-neural control system;
- We exclude the control effects of exteroception (sensing of external signals such as pressure) and vestibular system (it senses the angular velocity and the acceleration of the head). We believe that an inclusion of these effects should yield additional terms in our model such as, for instance, force feedback or a control term proportional to the measured acceleration;
- We assume a threshold value of the angle of the sway below which the motor-neural control of the proprioception is not applied, similarly as in [20]. This assumption is justified by the finite accuracy of sensing as well as by the recent finding of impulsive like control muscle movements reported in [18];

- We assume that the motor-neural control of the musculoskeletal system when sensing the error works like a PD control system with the time delay in the position and velocity error signals. The letter 'P' refers to the corrective torque that is proportional to the error signal between the desired angle θ_{ref} ($\theta_{\text{ref}} = 0$ in our case) and the measured angle multiplied by the proportionality factor, say K_p, that can be thought off as a stiffness factor. The letter 'D' refers to the corrective torque that is proportional to the velocity of the error signal between the desired velocity of the angle $\dot{\theta}_{\text{ref}}$ ($\dot{\theta}_{\text{ref}} = 0$ in our case) and the measured angular velocity with the proportionality factor, say K_d, that can be thought off as a damping factor.

Due to the presence of a threshold value our model is a hybrid (switched) system with time delay. The model we propose is similar to the one studied in [25] – the PD control is switched on or off depending on the value of state variables. The model studied in [25] is an extension of the studies conducted in [26, 27] where the authors introduce intermittently switched on/off controller that allows for a bounded motion, and it is this type of control which the authors in [25] propose as the possible explanation for the sway motion during quiet standing. The control strategy used in [25] is based on the assumption that a bang-bang control does not allow to produce sufficiently small bounded motion [27], with the sway angle of about one degree, which could correspond to the sway motion during quiet standing. In our paper we consider the simplest possible form of a dead-zone which is physiologically feasible, and we show in Sec. 4.4 that small scale stable periodic oscillations may be observed in bang-bang control systems in the presence of a dead-zone.

We briefly summarize the results of our investigations. To be able to maintain balance the control of the proprioceptive system must utilize both: (i) the information on the elongation and (ii) the information on the velocity of the elongation of the muscles. This agrees with the fact that to stabilize an inverted pendulum (for small angles θ when the linear model of the pendulum is assumed) a linear controller must at least use the proportional and derivative signals of the error. Stabilization is achieved through the existence of stable oscillations about an offset angle $\pm\theta_0$ where θ_0 corresponds to the size of the dead-zone. For a broad range of parameters these oscillations are accompanied by stable larger scale oscillations. The difference in the amplitude of the angle of larger scale oscillations in relation to smaller scale oscillations is at least two orders of magnitude. In the context of upright standing the small scale oscillations can be seen as a jitter about the nearly upright position; the ideal upright position cannot be achieved due to our assumption that the motor-neural control of the musculoskeletal system only reacts to values larger than the aforementioned offset angle $|\theta_0|$ which is physiologically determined. By adding white noise to our model equations we numerically show that close to a homoclinic bifurcation the system dynamics switches between two symmetric attractors. This scenario can explain noise-induced switchings between two coexisting attractors reported in [20]. Finally, we should note that multistability as well as the presence of periodic oscillations have already been reported in the literature on switched delay differential equations, see for instance [28, 29, 30, 31]. However, the delay differential equations studied in these works contain discrete time delay in the position feedback only.

The rest of the paper is outlined as follows. In Sec. 2 a class of systems of interest is introduced. The system without the time delay in control function is first studied in Sec. 3. We then go on to exploring the effects of time delay on system dynamics in Sec. 4. In the following Sec. 5 we introduce the modifications to the model that will be tested in the future. Finally, Sec. 6 concludes the paper.

2 The model equations

We simplify the biomechanics of the body by representing it as an inverted pendulum with the body sway occurring in the sagittal plane about the ankle joint axis. Gravity g acts on the centre-of-mass when the angle θ (measured in radians) between the vertical ankle joint axis and the body's position becomes non-zero; when there is no sway the body is vertical and $\theta = 0$. The centre of mass m is located at height h above the ankle joint axis.

We assume that to control the upright position a corrective torque T is applied through a PD controller when some fixed, but non-zero, positive threshold θ_0 is detected.

This leads to the following model equations:

$$J\ddot{\phi} = mgh\sin(\phi) \quad \text{for} \quad |\phi| \leq \phi_0, \tag{1}$$

when there is no control applied to the system, and

$$J\ddot{\phi} = mgh\sin(\phi) + T \quad \text{for} \quad |\phi| > \phi_0, \tag{2}$$

when the PD control is switched on; J is the moment of inertia of the body about the ankle joint axis. The delay terms are present in the applied torque generated by the PD controller. Namely

$$T = K_p\phi(t-\Delta_1) + K_d\dot{\phi}(t-\Delta_2), \tag{3}$$

where K_p and K_d are negative constants, and Δ_1, $\Delta_2 > 0$ are time delays.

We make a number of observations regarding the physical interpretation of the model. For $|\phi| \leq \phi_0$ the equations that govern system dynamics describe the dynamics of an inverted pendulum falling under the force of gravity. On the other hand for $|\phi| > \phi_0$ we have $J\ddot{\phi} = mgh\sin(\phi) + K_p\phi(t-\Delta_1) + K_d\dot{\phi}(t-\Delta_2)$. For $\Delta_1 = \Delta_2 = 0$ and $\sin(\phi) \approx \phi$ this equation is an equation of motion of a linear oscillator where the stiffness coefficient is given by $(-K_p - mgh) > 0$ and the damping by $-K_d > 0$. For Δ_1 and Δ_2 non-zero and positive we obtain a second order linear delay differential equation whose dynamics is significantly more complex than that of a second order linear oscillator [32, 33]. For sufficiently small Δ_1 and Δ_2, and under appropriate continuity assumptions, the dynamics of the delayed system can be studied using a set of ordinary differential equations [34]. However, the presence of switchings makes this reduction impossible even for small values of time delays.

Making the approximation $\sin\phi \approx \phi$, which is justifiable for small angles ϕ of the body sway, the model equations (1) and (2) become

$$\frac{J}{mgh}\ddot{\phi} = \phi \quad \text{for} \quad |\phi| \leq \phi_0, \tag{4}$$

and

$$\frac{J}{mgh}\ddot{\phi} = \phi + \frac{T}{mgh} \quad \text{for} \quad |\phi| > \phi_0. \tag{5}$$

To reduce the number of parameters we study system (4) and (5) in the non-dimensional form; we introduce the non-dimensional time $\bar{t} = \sqrt{\frac{g}{h}}t$ and set $\phi(t) = \theta(\bar{t})$, $x(\bar{t}) = \frac{d\theta(\bar{t})}{dt}$. Then $\dot{\phi}(t) = \dot{\theta}(\bar{t})\frac{\sqrt{g}}{\sqrt{h}}$ and $\ddot{\phi}(t) = \frac{g}{h}\ddot{\theta}(\bar{t})$ and we obtain

$$\ddot{\theta} = A\theta \quad \text{for} \quad |\theta| \leq \theta_0, \tag{6}$$

$$\ddot{\theta} = A\theta + \mathcal{T} \quad \text{for} \quad |\theta| > \theta_0, \tag{7}$$

where $A = \frac{mh^2}{J}$, $\mathcal{T} = B\theta(\bar{t} - \tau_1) + Cx(\bar{t} - \tau_2)$, with $B = \frac{hK_p}{gJ}$, $C = \frac{\sqrt{h}K_D}{\sqrt{g}J}$, $\tau_1 = \frac{\sqrt{g}}{\sqrt{h}}\Delta_1$, and $\tau_2 = \frac{\sqrt{g}}{\sqrt{h}}\Delta_2$. In what follows we drop the bar symbol when referring to non-dimensional time.

Setting $x = \dot{\theta}$ and using first order representation we arrive at a planar switched (Filippov) system of the form

$$F_{in} = \begin{pmatrix} \dot{\theta}(t) \\ \dot{x}(t) \end{pmatrix} = L \begin{pmatrix} \theta(t) \\ x(t) \end{pmatrix}, \qquad \text{for} \qquad |\theta| \leq \theta_0, \tag{8}$$

and

$$F_{out} = \begin{pmatrix} \dot{\theta}(t) \\ \dot{x}(t) \end{pmatrix} = L \begin{pmatrix} \theta(t) \\ x(t) \end{pmatrix} + \begin{pmatrix} 0 \\ B\theta(t-\tau_1) + Cx(t-\tau_2) \end{pmatrix} \qquad \text{for} \qquad |\theta| > \theta_0, \tag{9}$$

where

$$L = \begin{pmatrix} 0 & 1 \\ A & 0 \end{pmatrix}. \tag{10}$$

3 System dynamics for $\tau_1 = \tau_2 = 0$, and $\tau_1 \neq 0$, $\tau_2 = 0$

3.1 Switched system with no time delays

We start our investigations by discussing the dynamics of switched system (8) and (9) for $\tau_1 = \tau_2 = 0$. We first make the following observations:

1. Let $\mathbf{x} = (\theta,\ x)$ then, by the symmetry, we have that $-F_{in}(-\mathbf{x}) = F_{in}(\mathbf{x})$ and $-F_{out}(-\mathbf{x}) = F_{out}(\mathbf{x})$;

2. The integral curves of F_{in} are symmetric with respect to the θ and $\dot{\theta}$ axes.

Second observation implies that if an integral curve of F_{in} crosses the switching line Σ_1 at some point $a \neq 0$ then it either crosses $\Sigma_1 = \{\theta = \theta_0\}$, at $-a$ or $\Sigma_2 = \{\theta = -\theta_0\}$ at a. Similarly if we consider $a \in \Sigma_2$ then the integral curve either crosses Σ_2 at $-a$ or Σ_1 at a.

The only equilibrium of (8) and (9) is the origin or a pseudo-equilibrium. A pseudo-equilibrium of (8) and (9) is the equilibrium of the full system (8) and (9) that lies on the switching line Σ_1 or Σ_2.

For $A > 0$ the origin is an equilibrium of a saddle type characterized by the eigenvalues $\mu_1 = -\sqrt{A}$ and $\mu_2 = \sqrt{A}$ with the associated eigenvectors $\bar{\mu}_{\mathbf{1}} = [1,\ -\sqrt{A}]$ and $\bar{\mu}_{\mathbf{2}} = [1,\ \sqrt{A}]$.

Lemma 1 *Consider (8) and (9) with $A > 0$, and B and C negative, and such that $A+B < 0$. Then the only equilibrium of (8) and (9) is the origin. There are also two accumulation points (pseudo–equilibria) which are located at $(-\theta_0,\ 0)$ and $(\theta_0,\ 0)$. The origin is an equilibrium of a saddle type and the pseudo-equilibria are the only two global attractors of (8) and (9). The basins of attractions of these two pseudo-equilibria are separated by the piecewise-smooth invariant manifolds of the saddle point of the full system (8) and (9).*

Proof

The first part of the Lemma is trivial. The right-hand sides of (8) and (9) consist of sets of linear equations. If the determinants of matrix L given by (10) and the matrix

$$\begin{pmatrix} 0 & 1 \\ A+B & C \end{pmatrix}.$$

are non-zero, which is true for $A > 0$ and $A + B < 0$, then the only possible equilibria are located at the origin. It is vector field F_{in} that is defined in the neighbourhood of the origin. Then for $A > 0$ the equilibrium is of a saddle type as the eigenvalues of L are $\mu_1 = -\sqrt{A}$ and $\mu_2 = \sqrt{A}$. The only other possible equilibria are pseudo-equilibria which may only occur on the switching lines at points where the $\dot{\theta}$ component of vector fields F_{in} and F_{out} is 0. It is easy to verify that this is the case only at $(-\theta_0,\ 0)$ and $(\theta_0,\ 0)$.

To prove the second part of the lemma we first note that any point $(\theta,\ x)$ within the zone $|\theta| \leq \theta_0$ reaches some point on $\pm\theta_0$ in finite time at some point, say P_1. Let us suppose that P_1 lies on the positive part of Σ_1. From P_1 the flow follows the flow generated by F_{out} until some point $P_2 \in \Sigma_1$ is reached. The equations of motion along this segment of the flow are given by

$$\ddot{\theta} - (A + B)\theta = C\dot{\theta}.$$

Let $-(A + B) = \bar{A}$ and set $H = \left(\frac{1}{2}\dot{\theta}^2 + \frac{\bar{A}}{2}\theta^2\right)$, and multiply both sides by $\dot{\theta}$. We then have

$$\frac{d}{dt}H = C\dot{\theta}^2 < 0.$$

Thus P_2 must be closer to the origin than P_1. From P_2 the flow follows

$$\ddot{\theta} - A\theta = 0.$$

Using the energy argument again, and due to the fact that Σ_1 and Σ_2 are placed the same distance away from the origin, the energy at the next point of switching with Σ_1 or Σ_2 is the same as at P_2. There is a loss of energy only due to the application of the flow F_{out} and after subsequent switches between F_{in} and F_{out} the trajectory will converge to either of the two pseudo-equilibria since at these two points the system F_{out} reaches its lowest energy.

Finally, to determine which pseudo-equilibrium is reached we have to find the intersection points of the unstable and stable manifolds of the saddle point with Σ_i $(i = 1, 2)$. Concatenated segments joining subsequent intersection

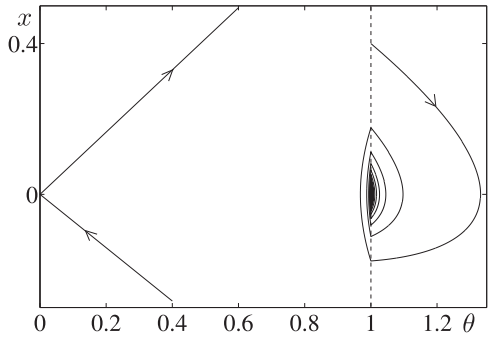

Figure 1: Illustrative trajectory of switched system (8) and (9) for $A = 0.5$, $B = -0.6$, $C = -0.5$, $\theta_0 = 1$, and the initial conditions $(\theta_0,\ x_0) = (1,\ 0.4)$ converging to a pseudo-equilibrium $(\theta_0,\ 0)$. The eigenvectors are depicted as solid lines.

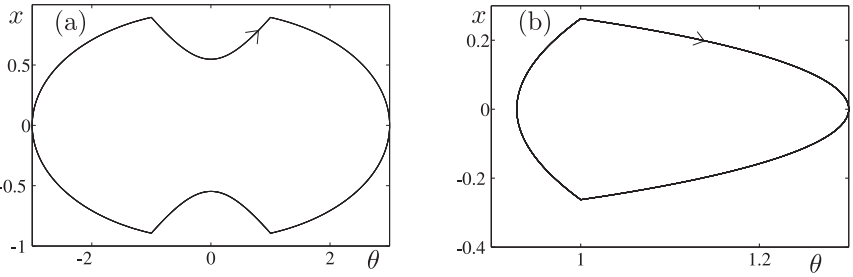

Figure 2: Periodic solutions of (8) and (9) for $A = 0.5$, $B = -0.6$ and $C = 0$ with no time delay, i.e., $\tau_1 = \tau_2 = \tau = 0$; (a) the initial conditions $(\theta_0,\ x_0) = [3,\ 0]$, and (b) $(\theta_0,\ x_0) = [1.3,\ 0]$.

points form piecewise-smooth stable and unstable manifolds. By considering the evolution of a single trajectory we can then show that the trajectory will be moving within a region bounded by the stable and unstable manifolds of the saddle point until it reaches either one of the two pseudo-equilibria. Due to system's symmetry if some point P_{In} converges to $(\theta,\ 0)$ then $-P_{In}$ will converge to $-(\theta,\ 0)$.

□

Illustrative trajectory of switched system (8) and (9) with $A = 0.5$, $B = -0.6$, $C = -0.5$, $\theta_0 = 1$, and the initial conditions $(\theta_0,\ x_0) = (1,\ 0.4)$ is depicted in Fig. 1.

If $A + B < 0$ and C is identically 0 it is easy to verify that our system exhibits an infinite number of periodic orbits which can be though of as centres. Two representative limit cycles for this case are depicted in Fig. 2.

If, on the other hand, $B = 0$ and $C < 0$ then the system trajectories will diverge to $\pm\infty$.

We conclude this section with the physical interpretation of our results. When both the proportional and derivative control is applied instantaneously

(no time delay due to sensing, processing and actuation) then provided that $A + B < 0$ it is possible to achieve perfect stabilization. However the angle θ at which the body is stabilized is offset from the vertical angle $\theta = 0$.

3.2 Effects of the damping term and the position delay ($\tau_1 \neq 0$ and $\tau_2 = 0$)

Our model system can be thought of as a generalisation of the model studied by Eurich and Milton in [20]. In this work the authors model human postural sway using a second order ordinary differential equation, which models inverted pendulum falling under the force of gravity, subject to time delayed restoring force and noisy perturbation. Using an assumption that the postural sway is overdamped, for healthy subjects with eyes open, they reduce their model to a first order system. Our numerics suggests that this reduction removes stable pseudo-equilibria present in the second order system. Thus, the reduced system does not have the possibility of producing multi-stabile behaviour in the sense of having more than one pair of stable asymmetric orbits; by the system's symmetry stable asymmetric orbits come in pairs.

We observed the existence of stable pseudo-equilibria in (8) and (9) with (8) having additionally a damping term $C\dot{\theta}(t)$. The switched system studied in this paper with the additional $C\dot{\theta}(t)$ term in (8), and with $\tau_2 = 0$, can be thought of a system with damping and delayed position feedback and it is then the full model system studied in [20]. Numerical results with B varied and fixed $A = 0.5$, $C = -10$, time delay $\tau_1 = 0.2$ and $\tau_2 = 0$ are shown in Fig. 3. In Fig. 3(a), for $B = 0.49$, the pseudo-equilibrium located at (1, 0) is unstable. We depict a representative diverging trajectory. A trajectory converging to a stable pseudo-equilibrium, existing for $B = 0.51$, is depicted in Fig. 3(b). The parameters are chosen so that the postural sway is overdamped. Reduction of this system to the first order will remove the possibility of having a stable pseudo-equilibrium which stable state may be of physiological importance.

4 Effect of time delay in the PD control

Time delay enters the model through the delay present in the PD controller. We assume that the time delay coming from the position and velocity signals are equal, that is, $\tau_1 = \tau_2 = \tau$. This simplifying assumption is justified because in reality we encounter distributed delays and there is no evidence that the delay coming from the position signal is significantly longer or shorter than the delay of the velocity signal.

To reduce the size of parameter space, for all our numerical experiments, we assume $\theta_0 = 1$. This assumption can be made without loss of generality as shown in the appendix (Sec. 7.1).

4.1 Characteristic equation of the delay system

To be able to understand the dynamics of our model we have to understand the effects of time delay on the dynamics of the control system (9). We can rewrite (9) as a second order linear retarded differential difference equation. We have

$$\ddot{\theta}(t) = A\theta(t) + B\theta(t-\tau) + C\dot{\theta}(t-\tau). \tag{11}$$

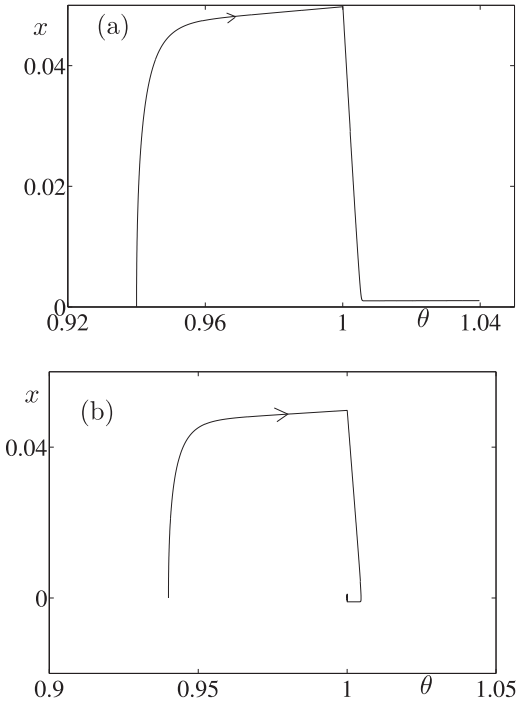

Figure 3: (a) Diverging trajectory in the switched system (8) and (9), modified by adding $C\dot{\theta}(t)$ within the dead zone, for $A = 0.5$, $B = -0.49$ and $C = -0.1$; time delay $\tau_1 = 0.2$, $\tau_2 = 0$. The initial history segment for the trajectory (for $t \in [-\tau,\ 0]$) is set to a constant value: $\theta(t) = 0.94$ and $x(t) = 0$. (b) Transient trajectory for $B = -0.51$ and other parameters as in (a) converging to a stable pseudo-equilibrium located at (1, 0). The initial history segment for the trajectory (for $t \in [-\tau,\ 0]$) is set to a constant value: $\theta(t) = 0.94$ and $x(t) = 0$.

Let $\theta(t) = \bar{c}\exp(\lambda t)$, where $\bar{c}$ is an arbitrary but non-zero constant. Then (11) becomes

$$\lambda^2 - A = B\exp(-\lambda\tau) + C\lambda\exp(-\lambda\tau). \tag{12}$$

Equation (12) is the characteristic equation of the retarded differential difference equation (11). The eigenvalue solutions λ of this equation determine the character of the solutions of (11).

4.2 Dynamics for $B = 0$ and τ small, and for $C = 0$ and τ small

Let us consider system dynamics when $C = 0$ and τ is small. Then the characteristic equation (12) becomes

$$\lambda^2 - A = B\exp(-\lambda\tau). \tag{13}$$

For $\tau = 0$ we obtain a system which conserves energy, and the eigenvalues of the characteristic equation of the ODE that governs system dynamics are $\lambda_{1,2} = \pm i\sqrt{|A+B|}$. For τ sufficiently small we calculate the dominant eigenvalues of the characteristic equation (13) by expanding it in τ. We then have

$$\lambda^2 = A + B(1 - \lambda\tau + \mathcal{O}(\tau^2)),$$

and after rearrangement we get

$$\lambda^2 + B\tau\lambda - (A+B) = \mathcal{O}(\tau^2). \tag{14}$$

Approximating the right-hand side of (14) to zero the roots of the quadratic equation (14) are

$$\lambda_{1/2} = \frac{-B\tau \pm \sqrt{B^2\tau^2 + 4(A+B)}}{2}.$$

By assumption $B < 0$, $(A + B) < 0$, and hence if $\tau > 0$ and sufficiently small there are at least two roots of (14) with positive real parts. This implies further that in the current case the trajectories of system (8) and (9) will diverge to infinity for τ sufficiently small. A representative trajectory for this scenario is depicted in Fig. 4 with the parameters set to $A = 0.5$, $B = -0.6$, $C = 0$, and time delay $\tau = 0.1$. We can similarly derive the approximate characteristic equation when $B = 0$ and $C < 0$, and argue that trajectories will diverge to infinity for τ sufficiently small.

To conclude

- If the derivative control is not active ($C = 0$: the damping term not present) or if the proportional control is not active ($B = 0$: no additional stiffness), and the time delay is small enough, the switched system (8) and (9) is not controllable, and all the trajectories diverge to $\pm\infty$;
- Numerics suggests that the above scenarios persist also for large values of τ.

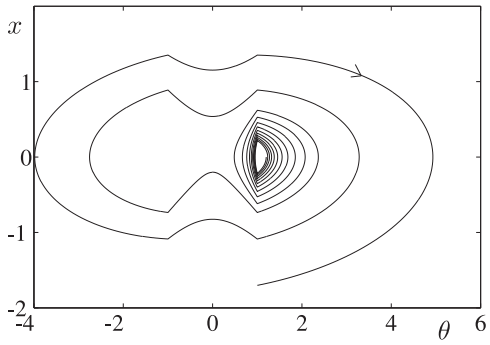

Figure 4: Representative trajectory of the switched system (8) and (9) for $A = 0.5$, $B = -0.6$ and $C = 0$; time delay $\tau = 0.1$. The initial history segment for the trajectory (for $t \in [-\tau,\ 0]$) is set to a constant value: $\theta(t) = 1.2$ and $x(t) = 0$.

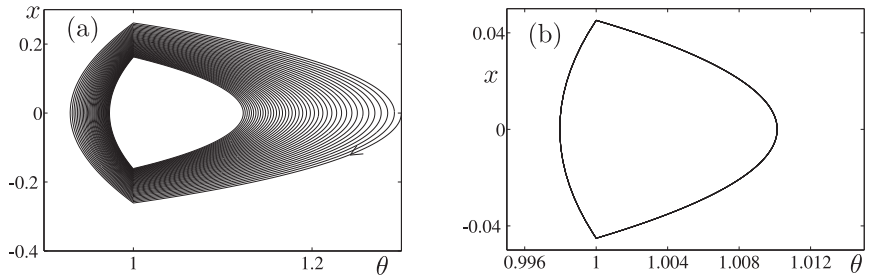

Figure 5: (a) A trajectory converging to an attractor of the switched system (8) and (9), for $A = 0.5$, $B = -0.6$ and $C = -0.07$; time delay $\tau = 0.1$, and (b) the attractor.

4.3 Switched PD control: B and C non-zero

To create a limit cycle it is necessary to move all the eigenvalues of the characteristic equation (12) to the left half-plane of the complex plane. Assume that both τ and C are small. To leading order in τ and C the characteristic equation (12) is

$$\lambda^2 - A = B + C\lambda - B\lambda\tau. \tag{15}$$

The two roots of the quadratic equation (15) are

$$\mu_{1,\,2} = \frac{1}{2}(C - B\tau \pm \sqrt{(B\tau - C)^2 + 4(A + B)}). \tag{16}$$

For C and τ sufficiently small these roots are complex conjugate, and it is the sign of the real part, that is the sign of $C - B\tau$, which determines if all the roots of the characteristic equation (12) lie in the left half-plane of the complex plane.

Considering the previous numerical example if we set $C = -0.07$ we expect that a system trajectory will converge to an attractor since then $C - B\tau < 0$,

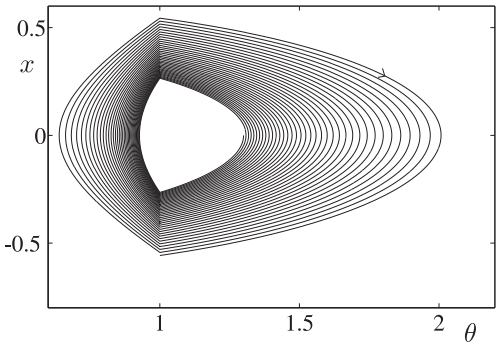

Figure 6: A diverging trajectory of the switched system (8) and (9) for $A = 0.5$, $B = -0.6$ and $C = -0.05$; time delay $\tau = 0.1$.

and the dominant eigenvalues lie in the left half-plane of the complex plane. This is indeed the case as depicted in Fig. 5.

In Fig. 6 we depict a diverging trajectory of (8) and (9) for $A = 0.5$, $B = -0.6$, $C = -0.05$ and the time delay $\tau = 0.1$. Hence the condition $C - B\tau < 0$ is violated and there exist eigenvalues of the characteristic equation (15) with a positive real part.

We should make a comparison here between our switched model and the delay differential equation that governs system dynamics outside of the dead zone. Assuming there is no dead zone (ideal sensing of the proprioceptive system) then the small scale stable oscillations present in the switched system correspond to the stable equilibrium states of the delay system. If, on the other hand, there are no attractors present in the switched system then the equilibrium of the delay system must be unstable, and the asymptotic dynamics of the switched and delay systems can be considered equivalent (the trajectories diverge to $\pm\infty$).

4.4 Multiple stable oscillations

Having established the existence of stable periodic oscillations in our model we wish to examine the region of parameter space where these oscillations persist, and also, what are the parameter values that are critical for the onset of different asymptotic dynamics. Initially we set the parameters to these values for which we found stable limit cycles in the previous section; we set $\tau = \tau_1 = \tau_2 = 0.1$, $A = 0.5$, $B = -0.6$, and we vary C. In Fig. 7(a) – Fig. 7(h) we are depicting representative limit cycles and corresponding time series for $C \in [-10, -0.1]$. We note that there is little effect of the variation of C on the amplitude and the period of the oscillations for $C \in [-10, -0.2]$ (see Fig. 7(c) – Fig. 7(h)). When we vary C between -0.2 and -0.1 we observe that the value of $\dot{x}$ at the switching between F_{in} and F_{out} increases from around 0.02 to 0.03 and the period from 0.5 to 0.7 (c.f. Fig. 7(c), (d) with Fig. 7(a), (b)). To sum up the effect of the variation of C on the existing periodic orbits is more pronounced for small values of C and there is little effect of the variation of C on the periodic orbits for $-10 < C < -0.2$.

To further investigate the system numerically we obtained one-parameter

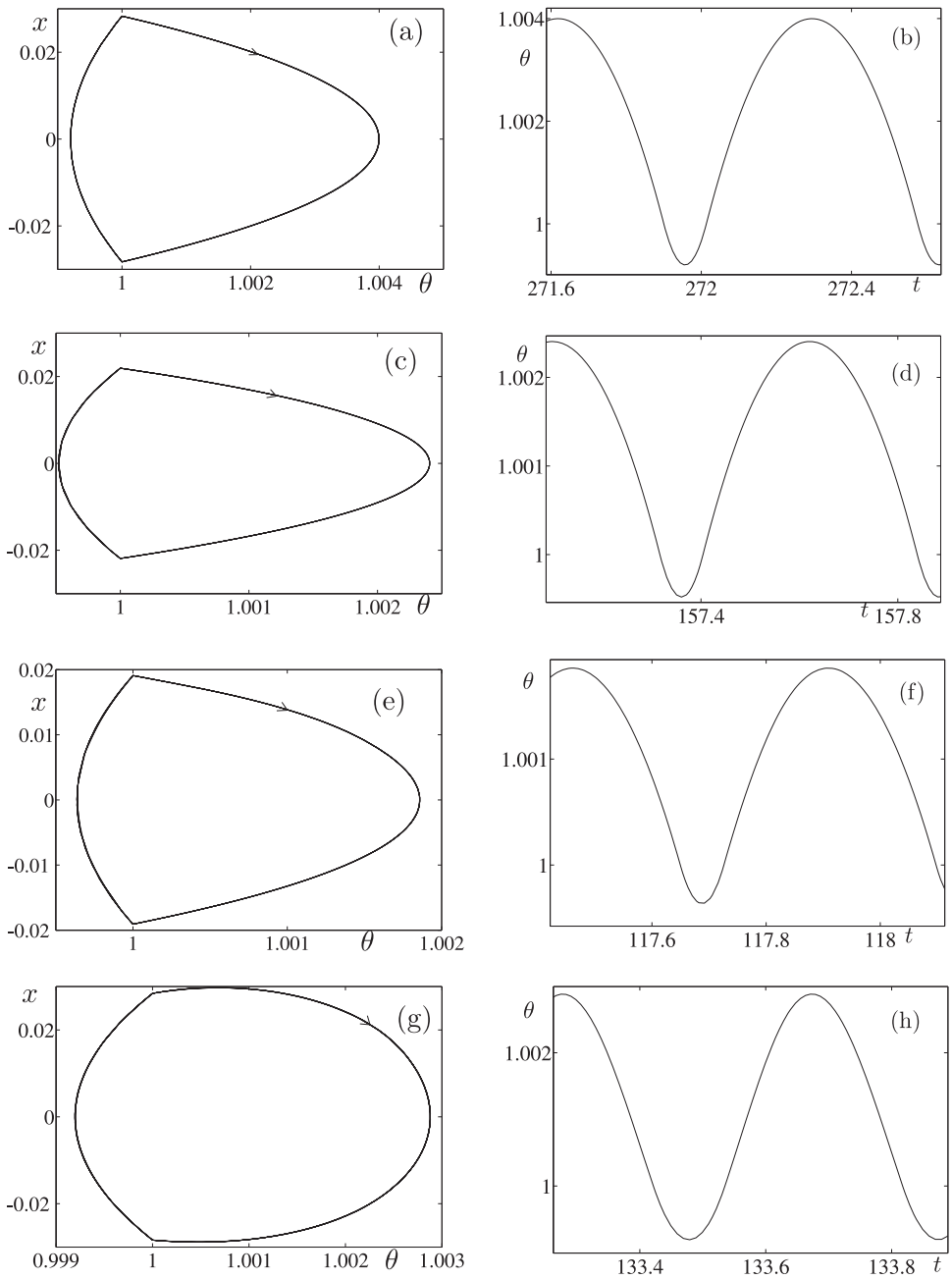

Figure 7: (a) Periodic orbits of the switched system (8) and (9) for $A = 0.5$, $B = -0.6$, $C = [-0.1(a), -0.2(c), -1(e), -10(g)]$ and the corresponding time series in (b), (d), (f) and (h). Time delay $\tau = 0.1$.

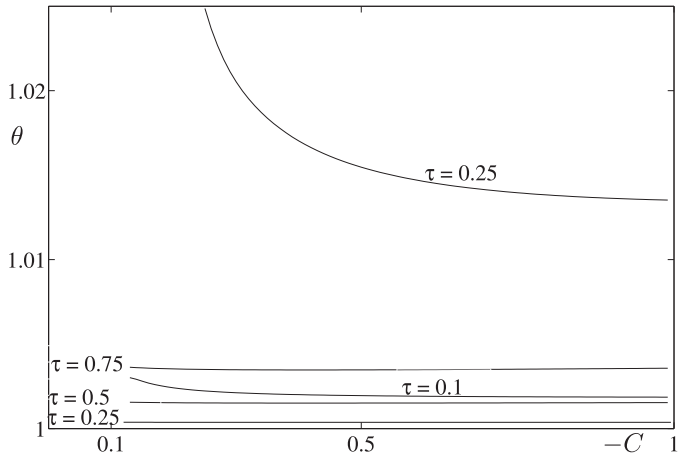

Figure 8: One parameter orbit diagrams capturing two families of periodic attractors. One family is characterized by negligible change in the amplitude for $C \in [-0.1, -1]$ (the values of τ are given to the left of the curves); the second family is characterized by a pronounced change in the amplitude for the values of C close to -0.1 (the values of τ are given above the curves).

orbit diagrams on which we depict the variation of a periodic point on the attractor versus parameter $-C$ for distinct values of the time delay τ, see Fig. 8. We found the co-existence of two families of attractors. Namely, we observe stable oscillations e.g. Fig. 7(a) – Fig. 7(h) that co-exist with stable oscillations of different period and amplitude. Note two curves obtained for $\tau = 0.25$ one in a close proximity of $x_1 = 1$ and the other further away from $x_1 = 1$.

We found the co-existence of these two families of attractors also for $\tau = 0.5$ and $\tau = 0.75$ (not depicted in the figure). We conjecture that these two families of attractors are born in the limit as $\tau \to 0$. Their presence is due to the switched nature of the system. Representative examples of two co-existing attractors, each corresponding to one family of periodic orbits, found for $\tau = 0.25$ are depicted in Fig. 9. The amplitude θ, say $Amp(\theta)$, of the limit cycle in Fig. 9(c) is $Amp(\theta) \approx 0.02$. This is about fifty times larger than $Amp(\theta)$ of the limit cycle in Fig. 9(a). The period of the limit cycle in Fig. 9(c) is about 1.2 which is approximately six time longer than the period of the limit cycle in Fig. 9(a); cf. the time series in Fig. 9(d) and Fig. 9(b).

4.5 Homoclinic bifurcations and bi-stability

Another important feature of our system is the birth of stable symmetric orbits with long period through so-called homoclinic bifurcation. This phase space transition takes place under increasing values of τ when the switching between F_{in} and F_{out} occurs at points on Σ_1 where the eigenvectors corresponding to the saddle point cross Σ_1.

Consider oscillations depicted in Fig. 10. Note that within the dead zone the orbit from Fig. 10(a) existing for $A = 0.5$, $B = -0.6$, $C = -1$ and $\tau = 1.1135$ is very close to the stable and unstable manifolds of the saddle point (note the

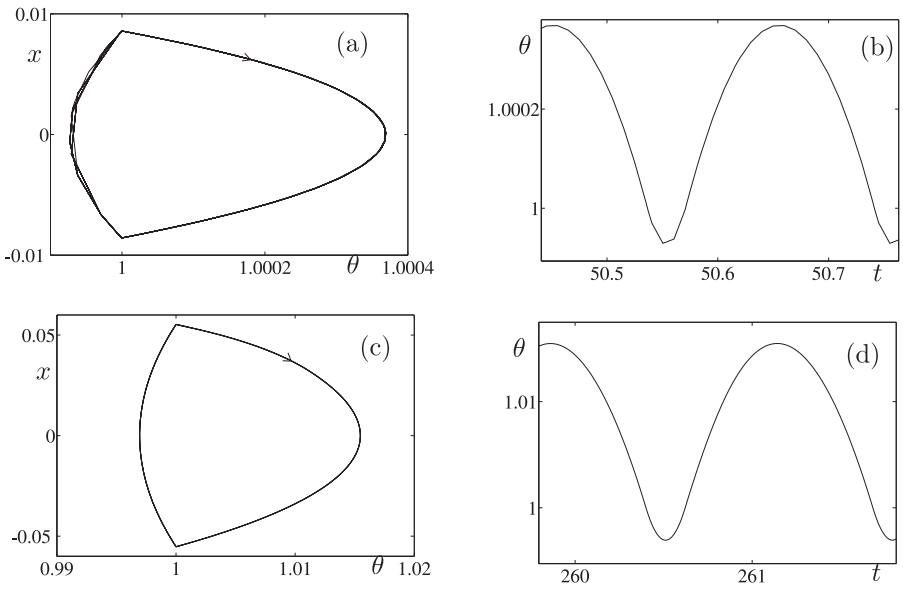

Figure 9: Co-existing stable limit cycles and corresponding time series of the switched system (8) and (9) for $A = 0.5$, $B = -0.6$ and $C = -0.5$. Time delay $\tau = 0.25$.

dashed lines in the figure superimposed on the orbit). For $\tau = 1.114$ this orbit no longer exists, instead a stable symmetric orbit born in the homoclinic bifurcation is present – see Fig. 10(c). A homoclinic orbit existing at the bifurcation is formed from the stable and unstable manifolds of the saddle point. Within the dead zone the shape of the orbit is given by the straight lines lying along the eigen-directions of the saddle point and outside of it by the arches joining these straight lines. In other words it is the stable and unstable manifolds that form a homoclinic orbit, and any trajectory starting its evolution on the orbit stays on it and reaches an unstable equilibrium of the saddle type in infinite time. This in turn implies that the periods of the orbits "before" and "after" the bifurcation are long – see time series in Fig. 10(b) and (d) respectively. The straight lines emanating from the origin refer to the stable and unstable eigen-directions of the saddle point. We believe that it is the homoclinic bifurcations which allows for the noise-induced switchings between two coexisting attractors reported in [20]. We note that sufficiently close to the bifurcation there exist two stable asymmetric attractors as depicted in Fig. 11(a). If we add white noise to the system then a typical trajectory will evolve around these two attractors as depicted in Fig. 11(b). In the latter case the switched system (8) and (9) becomes a stochastic switched system with time delay, and its evolution within the dead zone is governed by

$$F_{in} = L \begin{pmatrix} \theta(t) \\ x(t) \end{pmatrix} + \sigma\zeta(t), \qquad \text{for} \qquad |\theta| \leq \theta_0, \tag{17}$$

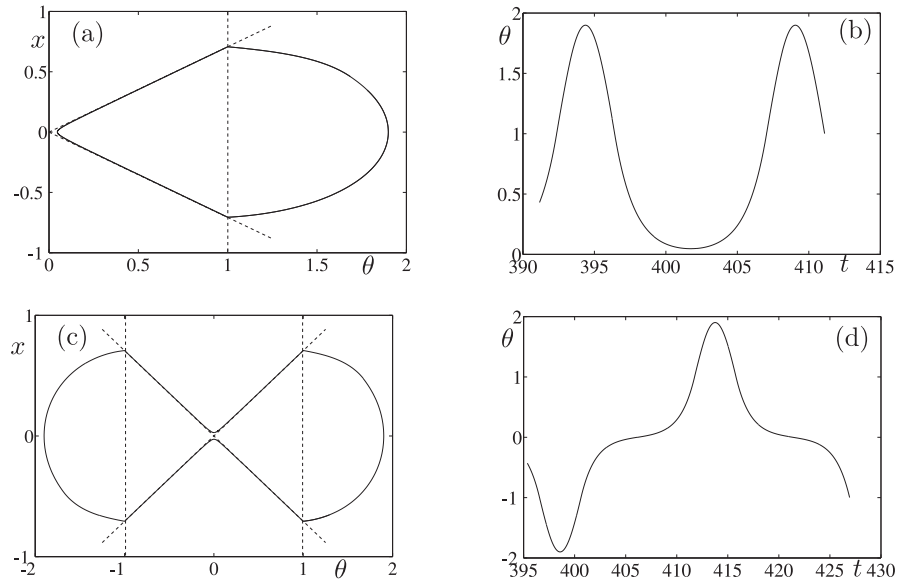

Figure 10: Homoclinic bifurcation for $A = 0.5$, $B = -0.6$, $C = -1$; (a) 'before' the bifurcation for $\tau = 1.1135$, in Fig. (b) we depict the corresponding time series, and (c) after the bifurcation for $\tau = 1.114$, in Fig. (d) we depict the corresponding time series.

and outside of the dead zone by

$$F_{out} = L \begin{pmatrix} \theta(t) \\ x(t) \end{pmatrix} + \begin{pmatrix} 0 \\ B\theta(t-\tau_1) + Cx(t-\tau_2) \end{pmatrix} + \sigma\zeta(t), \qquad \text{for} \qquad |\theta| > \theta_0, \tag{18}$$

where σ is the intensity of the applied white noise $\zeta(t)$. The parameter values are set to $A = 0.5$, $B = -0.6$, $C = -1$, $\sigma = 0.1$, and $\tau = 1.112$. Both figures were generated using first order Euler method with step size $\Delta t = 0.001$. The numerical integration scheme used to produce Fig. 11(b) is described in the appendix.

5 Modifications to the model

The investigations described here serve as an initial step to gain insight into the dynamics of upright balance. There is a number of modifications that could be considered to gain more insight into the problem of balancing. In the first instance we could alter the model with the dead zone and time delay to a model with time delay and delay in the switching function. This modification reflects our assumption on the presence of time delay in the neural transmission and muscle activation when switching the PD control. In the current paper we consider the simplest possible model and that is why the dead zone is fixed. This can also be seen as modelling the time delay in the neural transmission only. In some papers it is also argued that there is a time delay in the acceleration terms, see for instance [35]. It could be also interesting to compare different

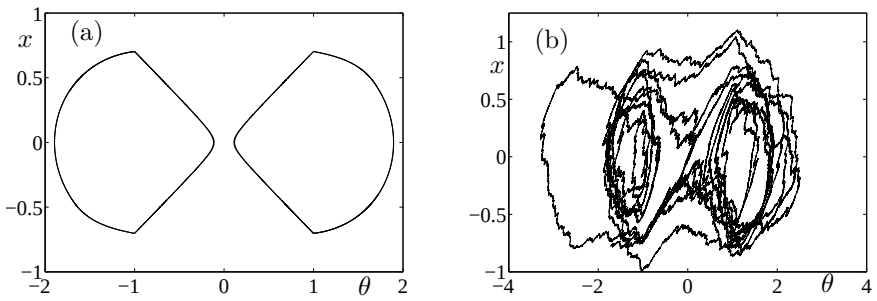

Figure 11: (a) Periodic attractors close to a homoclinic bifurcation of the switched system (8), and (b) a typical trajectory of the switched system (17) and (18) with added white noise.

control strategies and stable states that these can produce. Finally, we would like to develop the model to include the mechanism(s) of muscle tiring. This we believe to be a crucial element in the loss of balance in elderly people.

There are also other important issues. Namely the dynamics of a multiple link inverted pendulum model could be more realistic. These modifications will be pursued in collaboration with experimentalists who work on human balance.

At this point we would like to comment on the correspondence between the dimensional and nondimensional quantities of our model system. For example, if we take physiologically feasible values, similar to those used in [25], and set $m = 60kg$, $h = 1m$, $g = 9.81m/s^2$, $J = 60kgm^2$, time delay $\Delta_1 = \Delta_2 = 0.1s$, the width of the dead zone $|\theta| = 0.02rad$, and the control coefficients $K_p = 720Nm/rad$, $K_D = 60Nms/rad$ our nondimensional quantities are equal to $A = 0.0001$, $B = 0.00012$, $C = 0.0031$ and the time delay $\tau = 31$. Our numerical simulations show that for these parameter values the system exhibits stable pseudo-equilibria. We should note that these values are in a different regime from the one we explored numerically. The reason for our numerical exploration is that we want to discover all, or as much as possible, of qualitatively different dynamics that can be found in our model system. Having found multistability, small scale periodic oscillations, and a homoclinic bifurcation, all of which can be potentially important for human balance, it now remains to validate which of these scenarios can, indeed, be observed in experiments. This implies further that it may be necessary to use additional tools from dynamical systems analysis, for instance a numerical continuation of bifurcation curves, to obtain an exhaustive picture of the dynamics of the model system for parameter values which are physiologically feasible. However, this last point must be informed by experiments.

6 Conclusions

In the paper we introduce a model of human balance during quiet standing following the idea that a human body can be modelled by a single-link inverted pendulum, and balance is achieved using linear feedback control with time delay in the proportional and derivative error signals. We assume a threshold value of the angle of the sway below which the motor-neural control system cannot detect

any sway motion. We obtain a planar switched (hybrid) model. We find that to achieve stabilization, which is seen as 'small' oscillations about an upright equilibrium, it is necessary that both the proportional and derivative signals of the control system are used. These stable oscillations seem to represent closer to observation stable state for upright standing than the equilibrium points [23]. Therefore, we study the effects of parameter variations on their existence.

Our parameter study leads to the detection of a multiple number of stable oscillatory states existing for the same parameter values and for a wide range of the control parameter corresponding to the derivative term of the PD controller. We also find a homoclinic bifurcation that gives birth to a stable symmetric orbit with a long period. In particular, we show, using a numerical experiment, that close to a homoclinic bifurcation white noise introduced additively may result in the system switching between the two regions where symmetric stable solutions exist in the deterministic switched system leading to an apparent bi-stability; in other words, the switched system with added noise evolves for some time in the neighbourhood of each one of the two stable asymmetric limit cycles (present in the deterministic system) by switching between their regions of existence. This scenario can explain switchings between a pair of stable asymmetric attractors observed in the first order model in [20], which in turn was used to explain different scaling patterns that could be detected in human postural sway data.

Obviously, and important step in the investigations of human balance would be verification of the stable oscillatory states found in our model system. In particular, it would be interesting to see if, indeed, we can observe s small scale oscillations close to an equilibrium against the larger scale stable oscillations and how are these linked with the physiology of human subjects.

7 Appendix

7.1 Model scaling

Consider the system for $k > 0$ given by

$$\begin{aligned} \dot{\theta}(t) &= x(t), \\ \dot{x}(t) &= \begin{cases} \bar{A}\theta(t) & \text{if } |\theta| \le k \\ \bar{A}\theta(t) + \bar{B}\theta(t-\tau_1) + \bar{C}x(t-\tau_2) & \text{if } |\theta| > k, \end{cases} \end{aligned} \tag{19}$$

which is our standard control model with dead zone $|\theta| \le k$. We aim to show that this is equivalent (after scaling) to a model with dead zone $|\theta| \le 1$ of the form

$$\begin{aligned} \dot{\theta}(t) &= x(t), \\ \dot{x}(t) &= \begin{cases} \bar{A}k^2\theta(t) & \text{if } |\theta| \le 1, \\ \bar{A}k^2\theta(t) + \bar{B}k^2\theta(t-\frac{1}{k}\tau_1) + \bar{C}kx(t-\frac{1}{k}\tau_2) & \text{if } |\theta| > 1. \end{cases} \end{aligned} \tag{20}$$

Thus having a smaller dead zone (smaller k) corresponds, in systems rescaled so that the dead zone is constant, to having a larger relative dissipation but a longer delay time; i.e. the effect is not obvious (larger relative dissipation implies greater stability, longer delay implies less stability). Note that the time t in the second equation is not the same as the time t in the first equation.

To see this we will start from (20) and derive (19). First, let $\psi(t) = k\theta(t)$, so $|\theta| \leq 1$ becomes $|\psi| \leq k$ and $\frac{d\psi}{dt} = k\frac{d\theta}{dt}$ and (20) becomes

$$\begin{array}{rl} \dot{\psi}(t) & = kx(t), \\ \dot{x}(t) & = \left\{ \begin{array}{ll} \bar{A}k\psi(t) & \text{if } |\theta| \leq k, \\ \bar{A}k\psi(t) + \bar{B}k\psi(t - \frac{1}{k}\tau_1) + \bar{C}kx(t - \frac{1}{k}\tau_2) & \text{if } |\theta| > k. \end{array} \right. \end{array} \tag{21}$$

Now introduce a new time variable $u = kt$, and let $\phi(u) = \psi(t)$, and $y(u) = x(t)$. Note that

$$\psi(t - \tau) = \phi(k(t - \tau)) = \phi(u - k\tau), \tag{22}$$

and similarly for $y(u)$. Moreover

$$\frac{d\phi}{du}(u) = \frac{dt}{du}\frac{d}{dt}\psi(t) = \frac{1}{k}\frac{d}{dt}\psi(t),$$

and so using (21)

$$\begin{array}{ll} \frac{d\phi}{du}(u) & = \frac{1}{k}\dot{\psi}(t) = x(t) = y(u), \\ \frac{dy}{du}(u) & = \frac{1}{k}\dot{x}(t) = \bar{A}\psi(t) + \bar{B}\psi(t - \frac{1}{k}\tau_1) + \bar{C}x(t - \frac{1}{k}\tau_2) \ \text{ if } |\phi| > k, \end{array} \tag{23}$$

with a simpler equation if $|\phi| \leq k$. Finally using the definitions of ϕ and y, and the shift rule (22) gives (with primes denoting differentiation with respect to u)

$$\begin{array}{rl} \phi'(u) & = y(u), \\ y'(u) & = \left\{ \begin{array}{ll} \bar{A}\phi(u) & \text{if } |\phi| \leq k, \\ \bar{A}\phi(u) + \bar{B}\phi(u - \tau_1) + \bar{C}y(u - \tau_2) & \text{if } |\phi| > k, \end{array} \right. \end{array} \tag{24}$$

which is (19) after the identifications $\phi \to \theta$, $y \to x$ and $u \to t$.

7.2 Euler's method for the switched system with the time delay and white noise

Switched system (17) and (18) is a stochastic system with switching and time delay. The angle θ and the angular velocity $x = \dot{\theta}$ are now random variables. The presence of the switching function implies that depending on the value of the random variable θ system equation is governed by a stochastic differential equation, or a stochastic delay differential equation. We switch between these two systems when the random variable θ is greater or smaller than the threshold value θ_0. It has been shown in [36] that stochastic delay differential equations

$$\dot{x}(t) = f(x(t), x(t - \tau)) + \sigma\zeta(t), \tag{25}$$

where τ is the time delay, $\zeta(t)$ is Gaussian white noise with intensity σ, can be approximated by

$$x_{n+1} = x_n + f(x_n, x_{n-k})h + \sigma W_n\sqrt{h}, \tag{26}$$

for h sufficiently small; τ is the time delay, h is the step size, $k = \tau/h$, and W_n is the standard Wiener process. Similarly a stochastic differential equation

$$\dot{x}(t) = f(x(t)) + \sigma\zeta(t), \tag{27}$$

can be approximated by a discrete system

$$x_{n+1} = x_n + f(x_n)h + \sigma W_n \sqrt{h}. \tag{28}$$

Above numerical scheme was used to generate the trajectory of the stochastic switched system (17) and (18). Switching occurs at the integration step n when $\theta_n - \theta_0$ changes sign. The standard Wiener process is approximated numerically at each step t_n by a function that generates psudo-random numbers with expected value $\mu = \mathbf{E}[X] = 0$ and standard deviation $\sigma = \sqrt{\mathbf{E}[(X-\mu)^2]} = 1$, where X is a random variable.

References

[1] I. D. Loram, C. N. Maganaris, and M. Lakie. Paradoxical muscle movement during postural control. *Medcine in Science in Sports and Exercise*, 41:198–204, 2009.

[2] I. D. Loram, M. Lakie, M. D. Di Gulio, and C. N. Maganaris. The consequence of short range stiffness and fluctuating muscle activity for proprioception of postural joint rotations: the relevance to human standing. *Journal of Neurophysiology*, 2009.

[3] I. D. Loram, M. Lakie, and P. J. Gawthorp. Visual control of stable and unstable loads: what is the feedback delay and extent of linear time-invariant control ? *Journal of Physiology*, 587:1342–1365, 2009.

[4] M. D. Di Gulio, C. N. Maganaris, C. N. Baltzopoulos, and I. D. Loram. The proprioceptive and agonist roles of gastrocnemius, soleus, and tibialis anterior muscles in maintaining human upright posture. *Journal of Physiology*, 587:2399–2416, 2009.

[5] R. J. Peterka. Sensorimotor integration in human postural control. *Journal of Neurophysiology*, 88:1097 – 1118, 2002.

[6] R. J. Peterka and P. J. Loughlin. Dynamic regulation of sensorimotor integration in human postural control. *Journal of Neurophysiology*, 91:410 – 423, 2004.

[7] J. Jeka, T. Kiemel, R. Creath, F. Horak, and R. Peterka. Controlling human upright posture: Velocity information is more accurate than position or acceleration. *Journal of Neurophysiology*, 92:2368 – 2379, 2004.

[8] Ch. Maurer and R. J. Peterka. A new interpretation of spontaneous sway measures based on a simple model of human postural control. *Journal of Neurophysiology*, 93:189 – 200, 2005.

[9] M. Cenciarini and R. J. Peterka. Stimulus-dependent changes in the vestibular contribution to human postural control. *Journal of Neurophysiology*, 95:2733 – 2750, 2006.

[10] A. D. Goodworth and R. J. Peterka. Contribution of sensorimotor integration to spinal stabilization in humans. *Journal of Neurophysiology*, 102:496 – 512, 2009.

[11] A. D. Goodworth and R. J. Peterka. Influence of stance width on frontal plane postural dynamics and coordination in human balance control. *Journal of Neurophysiology*, 2010.

[12] P. Gatev, S. Thomas, T. Kepple, and M. Hallett. Feedforward ankle strategy of balance during quiet stance in adults. *Journal of Physiology*, 514:915–928, 1999.

[13] D. A. Winter, A. E. Patla, F. Prince, M. Ishac, and K. Gielo-Perczak. Stiffness control of balance in quiet standing. *Journal of Neurophysiology*, 80:1211–1221, 1998.

[14] D. A. Winter, A. E. Patla, A. E. Riedtyk, and M. Ishac. Ankle muscle stiffness in the control of balance during quiet standing. *Journal of Neurophysiology*, 85:2630–2633, 2001.

[15] K. Masani, M. R. Popovic, K. Nakazawa, K. Kouzaki, and D. Nozaki. Importance of body sway velocity information in controlling ankle extensor activities during quiet stance. *Journal of Neurophysiology*, 90:3774–3782, 2003.

[16] R. J. Peterka. Simplifying the complexities of maintaining balance. *IEEE Engineering in medcine and biology magazine*, pages 63–68, 2003.

[17] K. Craik. Theory of the human operator in control systems: I. the operator as an engineering system. *British Journal of Psychology*, Gen Sect 38:56–61, 1947.

[18] I. Loram, P. Gawthrop, and M. Lakie. The frequencey of human, manual adjustments in balancing an inverted pendulum is constrained by intrinsic physiological factors. *The Journal of Physiology*, 557(1):417–432, 2006.

[19] I. Loram, H. Gollee, M. Lakie, and P. Gawthrop. Human control of an inverted pendulum: Is continuous control necessary? is intermittent control effective? is intermittent control physiological? *The Journal of Physiology*, 589(2):307–324, 2011.

[20] Ch. Eurich and J. Milton. Noise-induced transitions in human postural sway. *Physical Review E*, 54(6):6681–6684, 1996.

[21] J. Milton, J. Cabrera, and T. Ohira. Unstable dynamical systems: delay, noise and control. *EPL*, 83(4):48001, 2008.

[22] J. Milton, T. Ohira, J. Cabrera, R. Fraiser, J. Gyorffy, F. Ruiz, M. Strauss, E. Balch, P. Marin, and J. Alexander. Balancing with vibration: A prelude for "drift and act" balance control. *PloS ONE*, 4(e7427), 2009.

[23] J. Milton, J. L. Cabrera, T. Ohira, S. Tajima, Y. Tonosaki, C. W. Eurich, and S. A. Campbell. The time-delayed inverted pendulum: Implications for human balance control. *Chaos*, 19(2), 2009.

[24] J. Milton, J. L. Townsend, M. A. King, and T. Ohira. Balancing with positive feedback: the case for discontinuous control. *Philosophical Transactions of the Royal Society A*, 367:1181–1193, 2009.

[25] Y. Asai, Y. Tasaka, K. Nomura, T. Nomura, M. Casadio, and P. Morasso. A model of postural control in quiet standing: Robust compensation of delay-induced instability using intermittent activation of feedback control. *PLoS ONE art. no. e6169*, 4(7), 2009.

[26] A. Bottaro, M. Casadio, P. Morasso, and V. Sanguineti. Body sway during quiet standing: Is it the residual chattering of an intermittent stabilization process? *Human Movement Science*, 24:588615, 2005.

[27] A. Bottaro, Y. Yasutake, T. Nomura, M. Casadio, and P. Morasso. Bounded stability of the quiet standing posture: An intermittent control model. *Human Movement Science*, 27:473495, 2008.

[28] U. an der Heiden, A. Longtin, M. Mackey, J. Milton, and R. Scholl. Optimal sensorimotor transformations for balance. *Journal of Dynamics and Differential Equations*, 2(4):423–449, 1990.

[29] U. an der Heiden and M. Richard. Multitude of oscillatory behaviours in a nonlinear second order differential-difference equation. *Journal of Applied Mathematics and Mechanics*, 70:621–624, 1992.

[30] W. Bayer and U. an der Heiden. Delay-differential equations with discrete feedback: explicit formulae for infinitely many coexisting periodic solutions. *Journal of Applied Mathematics and Mechanics*, 87:471–479, 2007.

[31] W. Bayer and U. an der Heiden. Oscillation types and bifurcations of a nonlinear second-order differential-difference equation. *Journal of Dynamics and Differential Equations*, 10(2):303–326, 1998.

[32] G. Stépán. *Retarded Dynamical Systems: Stability and Characteristic Functions*. Longman Sc and Tech, 1990.

[33] J. K. Hale and S. M. V. Lunel. *Introduction to Functional Differential Equations*. Springer, Springer-Verlag New York, 1993.

[34] C. Chicone. Inertial and slow manifolds for delay equations with small delays. *Journal of Differential Equations*, 190:364–406, 2003.

[35] D. Lockhart and L. Ting. Oscillatory modes in a nonlinear second-order differential equation with delay. *Nature Neuroscience*, 10(4):1329–1336, 2007.

[36] P. E. Kloeden and E. Platen. *Numerical Solution of Stochastic Differential Equations*. Springer-Verlag, 1995.

Acknowledgements
Research partially funded by Engineering and Physical Sciences Research Council grant EP/E050441/1 (CICADA: Centre for Interdisciplinary Computational and Dynamical Analysis), the University of Manchester and Manchester Metropolitan University.